Silicon (2022) 14:5923–5929
https://doi.org/10.1007/s12633-021-01370-3

ORIGINAL PAPER

Characterization Properties of Diopside Glass ($Cu_{0.50}Ca_{0.75}Mg_{0.75}Si_2O_6$) Containing Cr_2O_3 or TiO_2

Reham M.M. Morsi[1] · Gehan T. El-Bassyouni[2] · Esmat M. A. Hamzawy[3]

Received: 28 June 2021 / Accepted: 31 August 2021 / Published online: 12 September 2021

Abstract

The characterization of diopside –based glass of the composition $Cu_{0.50}Ca_{0.75}Mg_{0.75}Si_2O_6$ containing small additions of Cr_2O_3 or TiO_2 was explored. The techniques used for the characterization process include AC conductivity (σ_{ac}), X-ray diffraction (XRD) and Scanning electron microscopy (SEM). However, the prepared dark green glasses show very little devitrification of traces diopside, cuprite and tenorite. The SEM shows a massive structure at the nanoscale with little scattered clusters of nano crystals of the latter phases**.** The σ_{ac} was measured within the frequency range of 0.042 kHz −1 MHz and at the temperature range of 298–573 (K). The electrical conductivity measurements proved that the incorporation of Cr_2O_3 and TiO_2 results in higher conductivity values than those of the free glass sample. The activation energy of each of these glasses was estimated at high temperature range. The calculated activation energy values measured at 100 kHz and 1 MHz of the glass samples lie in the range 0.55–0.98 (eV). The prepared glass samples exhibited semiconducting nature.

Keywords Cu- containing glass · Devitrification · Electrical properties · Diopside glass

1 Introduction

Diopside ($MgCaSi_2O_6$) is a monoclinic prismatic mineral that arranges in a patchily colored patter. However, it frequently has a dull green clear to translucent crystals [1]. Diopside of interlaced structure; encompasses chain structure. The benefits of the core crystal phase with diopside have good mechanical properties, chemical stability, and the crystallization ability of pyroxene is remarkable [2]. Diopside based glass has numerous exceptional properties, such as chemical and mechanical properties [3–5]. The bases of raw materials are different, and its preparation is simple. The adding of operative nucleating agents such as Cr_2O_3 and TiO_2 [6–9] could be used for epitaxial growth, to tempt the precipitation of diopside, in the CaO–MgO–Al_2O_3–SiO_2 (CMAS) glass ceramics. The role of the nucleating agents must be elucidated [10]. In 2016, Sycheva et al., reflected that spinel ($MgCr_2O_4$) or spinel-like solid solution (Mg, Fe) (Al, Fe, Cr)$_2O_4$, can be used as the basic of diopside ($CaMgSi_2O_6$) crystallization [11]. Depending on the high chemical stability of diopside and its coefficient of thermal expansion, diopside ($CaMgSi_2O_6$) based glass have been known as promising materials for solid oxide cell (SOC) sealing applications [12, 13]. Liu et al. emphasized that amorphous metal oxide semiconductors are of essential and technological interest owing to their high carrier mobility and large-area uniformity [14]. Differential thermal analyses, X-ray diffraction, scanning electron microscopy as well as physical and dielectric properties were used to characterize and investigate the influence of the Cr_2O_3 content on the structure and properties of glass ceramics [15]. The heat treatment temperature and the percentage of TiO_2 were found to affect the microwave dielectric properties of the glass-ceramic composite material, where the dielectric constant was influenced by the crystallite size and the TiO_2 content [16]. The addition of Cr_2O_3 into glass ceramic was found to affect the crystallization, flexural strength, microstructure, thermal expansion, and the electrical properties [17]. The nanostructure/ microstructure of diopside based glass ceramics have been studied by several authors [18–20]. It was reported that by varying the composition of some

✉ Reham M.M. Morsi
morsi_reham@yahoo.com

[1] Physical Chemistry Department, National Research Centre, 33 El Buhouth St, Dokki, Giza 12622, Egypt

[2] Refractories, Ceramics and Building Materials Department, National Research Centre, 33 El Buhouth St, Dokki, Giza 12622, Egypt

[3] Glass Department, National Research Centre, 33 El Buhouth St, Dokki, Giza 12622, Egypt

diopside ceramics, the electrical conductivity and the glass phase of the achieved material can be controlled [21].

The objective of this study was to characterize diopside – based glass of the ternary system SiO_2-CaO-MgO modified with CuO and including small additions of Cr_2O_3 or TiO_2 using AC conductivity. The prepared material was examined by XRD, and the morphology was observed by SEM.

2 Experimental

2.1 Glass Preparation and Characterization

The present glasses are based on diopside ($Cu_{0.50}Ca_{0.75}Mg_{0.75}Si_2O_6$; (CaO = MgO) with the substitution of Cu for Ca and Mg. The glass batch was prepared from silica sand, carbonates of Ca and Mg; pure CuO. Little pure Cr_2O_3 and TiO_2 were added too (Table 1). The glass batches were weighed, mixed, melted and homogenized in Pt crucibles. The melting process was carried out in electrical globar furnace at 1400–1450 °C. Each melt was poured into a steel mold, and the cast pieces of viscous glass melts were annealed at 450 °C.

Powder X-ray diffraction (XRD-model-Bruker AXS D8 advance using Cu Kα- radiation) was used to test the glass. However, the glass samples were ground to powder with an average size below 63 μm and XRD patterns. The microstructure of the glass samples was studied via scanning electron microscopy to sure of the phases precipitated (SEM/EDX - Philips-XL30). For examination on the SEM, the fresh fracture glass samples were etched in 1% HF + 1%HNO_3 for 30 s and then rinsing with distilled water. Before SEM observation, all specimens were coated with a thin film of carbon.

2.2 Electrical Measurements of the Glasses

The AC conductivity (σ_{ac}) of the prepared samples was measured using LRC Hi-Tester (HIOKI, 3532–50) Japan, over a frequency range from 0.042 kHz to 1 MHz and temperature range from 298 to 573 (K). Increasing the temperature was provided by increasing the input voltage of a variac transformer connected to a wire-wound resistance heater. The temperature was determined using a copper/Constantine thermocouple in close proximity to the sample. The capacitance, C, and the dissipation factor, $tan\ \delta$, are obtained directly from the instrument for the studied samples. The AC conductivity, σ_{ac}, is calculated using the relation [22].

$$\sigma_{ac} = \omega\varepsilon_o\ \varepsilon^{'} tan\delta,$$

where ω = the angular frequency, ε_o = the permittivity of free space equals 8.85 × 10^{-12} F m^{-1} and ε' = the dielectric constant which is determined from the expression: $\varepsilon' = C\ d\ /\ \varepsilon_o A$, where d = thickness of the sample (m) and A = Sample surface area (m^2) [23].

3 Results and Discussion

3.1 Glass Characterization

The as-received G0, G0.5Cr and G5T transparent glass samples showed no devitrification with the naked eyes. However, the X-ray diffraction analysis shows very clear amorphous hump which reflects the glass transparency as well; also little weak lines represent the devitrification of diopside with copper oxide minerals, i.e. cuprite Cu_2O (JCPDS file No.05–0667) and tenorite CuO (JCPDS file No.05–661) in addition to traces of Cristobalite as revealed in Fig. 1. It has been reported that at high temperature CuO undergoes a redox reaction which result in the formation of Cu^+ ions [24]. The slow cooling of the glass melts with copper in high quantity has the ability to deposit it in the glass.

The SEM of freshly glass surfaces shows a massive structure at the nanoscale in all the samples that reflect the role of copper in the glass composition. The SEM of freshly glass surfaces shows a massive nanostructure in all the samples. Figure 2 shows the effect of the supersaturation of CuO (17%) in the diopside glass studies due to the slow rate of cooling. We can easily notice that, at high magnification of all the samples, there are tiny crystals and clusters in nanometer size (50–200 nm) scattered in the matrix.

Table 1 Composition of the glass batches and the product

Sample No	Chemical composition Constituent				Addition in gm Over 100% glass oxides		Melting Temperature °C	Product
	SiO_2	CaO	MgO	CuO	Cr_2O_3	TiO_2		
G0	51.75	18.12	13.02	17.13	–	–	1400	Transparent dark green glass
G0.5Cr	51.75	18.12	13.02	17.13	0.5	–	1450	Transparent dark green glass
G5T	51.75	18.12	13.02	17.13	–	5	1450	Transparent dark green glass

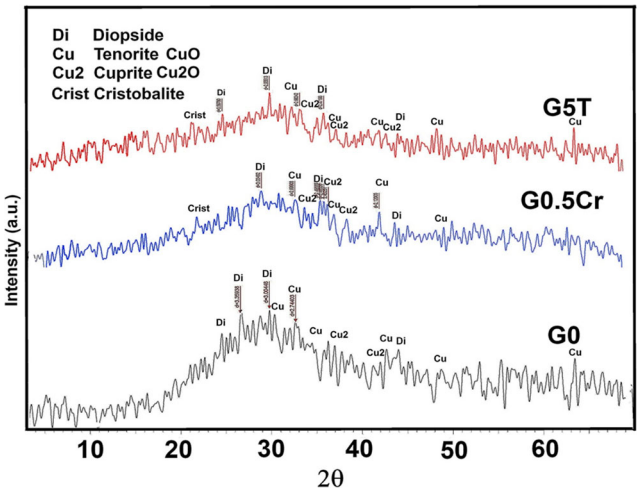

Fig. 1 X-ray diffraction patterns of as received glasses that show very little devitrification

For the glass samples, Fig. 3 (a, b and c) shows the change of log (σ_{ac}) with the reciprocal of temperature at several frequencies. It found that the conductivity increases with rising temperature for the glass samples in all the temperature range investigated which reveals that the present samples are semiconducting in nature [25, 26]. This rising of conductivity with temperature may indicate that the σ_{ac} is a thermally activated mechanism [27].

The activation energies were estimated from the slopes of the log σ plots versus 1000 / T plots at the two frequencies 100 kHz and 1 MHz (Table 2).The activation energy values are found to be in the range 0.55–0.98 (eV) at high temperature region from 473 to 573 (K). It could be observed that the activation energy of all glasses shows a decrease with increasing of frequency. This decrease can be connected with rising the applied frequency, increasing the movement of mobile ions between localized states [28] and increasing of electron hopping between the localized states [29].

From Fig. 3 (b and c) it can be noticed that, the σ_{ac} of the samples G0.5Cr and G5T is increasing nonlinearly with increasing the measuring temperature and exhibiting two regions. This behavior is valid for the higher and the lower frequencies. The two regions are formed by two different mechanisms, the first at the low temperature and the second at the high temperature regions. The first one is characterized

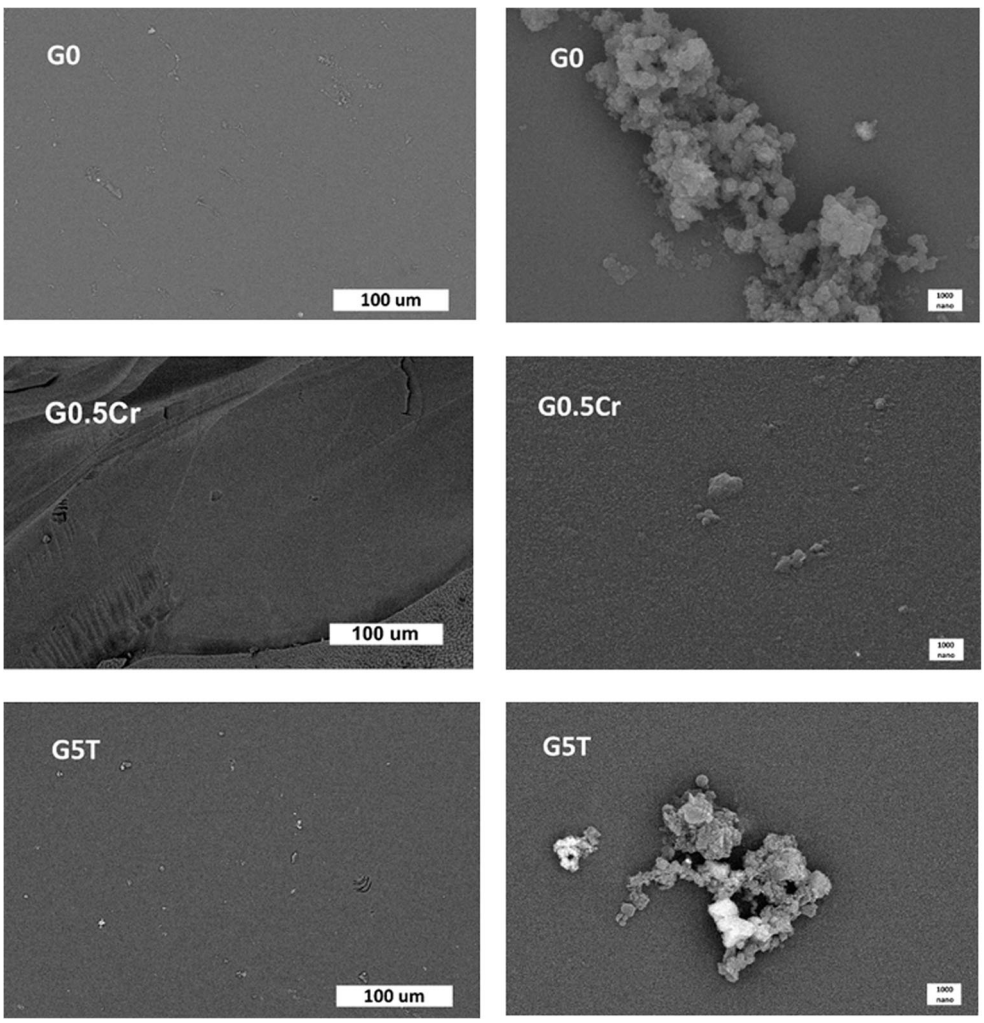

Fig. 2 Scanning electron microscopy of the as received glasses that show very little devitrification

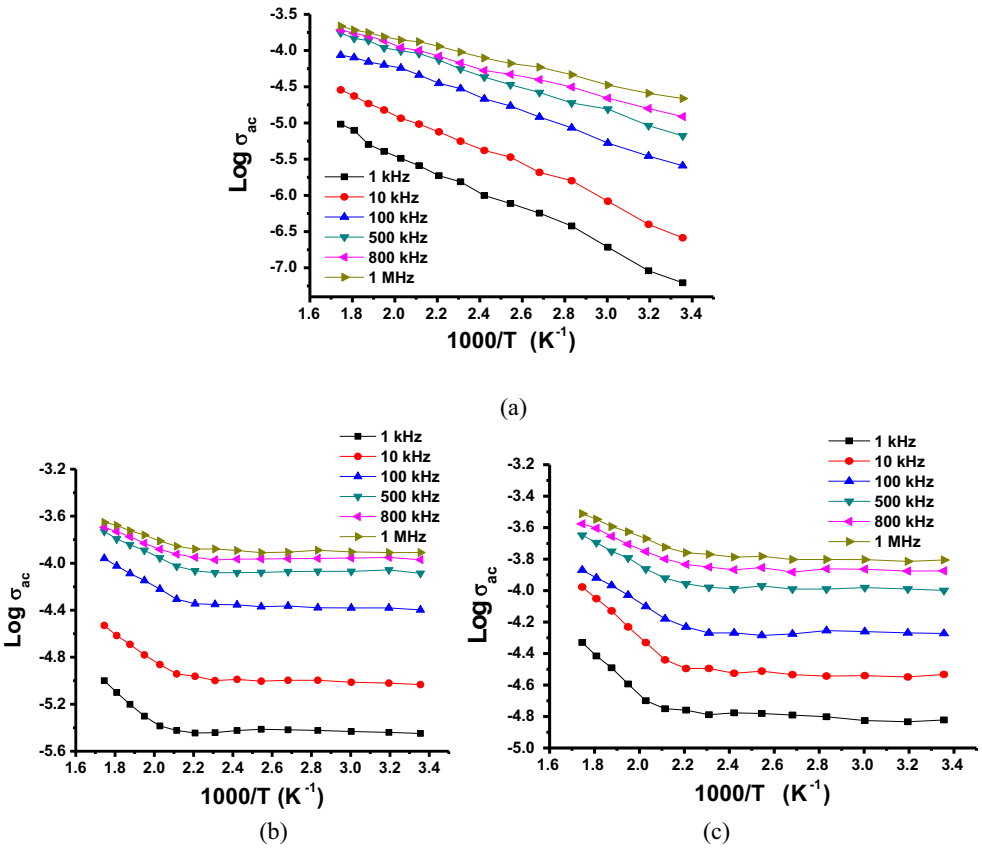

Fig. 3 Variation of AC conductivity (σ_{ac}) with the inverse of temperature at different frequencies for all samples

by low activation energy and low slope due to electronic transition mechanism, while the second one is characterized by higher activation energy and higher slope as results of participation of ionic movement mechanism. In the low temperature region, the conductivity slightly rises with temperature, which can be attributed to electronic mechanism arising from electronic transition between Cu^{+} and Cu^{+2}. The presence of Cu^{+} ions in Cu-containing glass is reported in silicate glasses [30]. Furthermore, both Cu^{+} and Cu^{2+} are reported to exist at temperature above 1250 °C due to the redox reaction:

$Cu^{2+} + ½O_2 \leftrightarrow Cu^{+} + ¼\ O_2$, which may explain the formation of Cu^{+} ions [24]. The electronic mechanism can also be carried out by the electronic transition between Ti^{+3} and Ti^{+4} which may exist in case of sample G5T or between Cr^{3+} and Cr^{6+} in sample G0.5Cr. However, it was found that both Cr (II) and Cr (III) exist simultaneously in CaO-MgO/Al_2O_3-SiO_2-CrOx system [31]. The presence of multivalent states for Cr permits the electronic transition between these states of Cr and contributes in the total Cr in the melt of the glass [32]. The transfer of these electrons could be considered as a small polarons hopping process [22, 33]. In the high temperature region, *log* σ_{ac} increases with a higher rate which may be attributed to the participation of ions coming from the increase in the formation of Cu^{+2}, as some Cu_2O may transferred by oxidation to CuO at higher temperature. In addition to this mechanism, the mobility of the charge carriers Ca^{+2} and Mg^{+2} ions may play a role in the conductivity [34, 35].

On the other hand, we can notice from Fig. 3a that the σ_{ac} increases linearly with increasing the temperature for the sample G0. This behavior and the high values of activation energy (E_a) (Table 2) can be attributed to predominant of ionic mechanism arising from Cu^{+2} in addition to the mobility of the

Table 2 The values of AC conductivity (σ_{ac}) and the activation energy (E_a) at different frequencies

Sample No.	E_a (eV), 100 kHz	E_a(eV), 1 MHz	$\sigma_{ac}(Sm^{-1})^a$, 100 kHz	$\sigma_{ac}(Sm^{-1})^b$, 100 kHz	$\sigma_{ac}(Sm^{-1})^a$, 1 MHz	$\sigma_{ac}(Sm^{-1})^b$, 1 MHz
G0	0.98	0.62	2.57×10^{-6}	8.62×10^{-5}	2.18×10^{-5}	2.17×10^{-4}
G0.5Cr	0.91	0.56	4.00×10^{-5}	1.10×10^{-4}	1.23×10^{-4}	2.22×10^{-4}
G5T	0.80	0.55	5.34×10^{-5}	1.35×10^{-4}	1.56×10^{-4}	3.08×10^{-4}

[a] Measured at room temperature, [b] Measured at 573 K

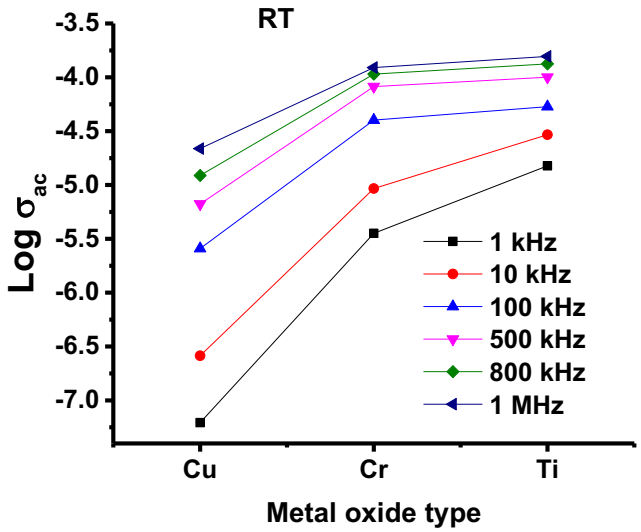

Fig. 4 Variation of AC conductivity as a function of type of metal oxide of all samples measured at room temperature and different frequencies

charge carriers (Ca^{+2} and Mg^{+2} ions) [35, 36], The slopes of the curves in this case seems different from those in Figs. 3b and 3c which can be attributed to the absence of electronic mechanisms caused by titanium and chromium ions.

Figure 4 presents the change in the AC conductivity, measured at different frequencies and at room temperature, depending on the type of metal oxide. From this figure, the results obtained showed that the introduction of Cr_2O_3 and TiO_2 led to an increase in the electrical conductivity of the glass sample G0. This behavior applies to all frequencies. For example, the σ_{ac} increases at room temperature and 100 kHz from 2.57×10^{-6} S/m for sample G0 to 4.01×10^{-5} and 5.34×10^{-5} (S/m) for samples G0.5Cr and G5T, respectively. As the temperature rises to 573 K, the values of the AC conductivity of the samples increase in the same manor (Table 2). It is reported that, semiconductors have conductivity values between 10^{3} and 10^{-8} $S.cm^{-1}$ [37]. The studied samples exhibited room temperature conductivity values in the range 10^{-8} - 10^{-4} S/m at the studied frequency range; therefore, they can be considered as semiconducting materials.

Figure 5 illustrates the frequency dependence of the alternating-current conductivity (σ_{ac}) at room temperature (Fig. 5a) and at 573 K (Fig.5b), in the frequency range extending from 0.042 kHz to 1 MHz and for all samples under investigation. It can be observed that the conductivity σ_{ac} increases with increasing frequency, which implies that the present glass samples are of semiconducting nature [38]. The measured conductivity, σ, can be considered as a summation of the DC conductivity, σ_{dc}, and AC conductivity, σ_{ac}. The DC part is independent of frequency, is dominant at low frequencies and appears as a flat DC plateau at low-frequency region. It is generally known [39] that AC conductivity depends on the polarization of immobile ions (silica network) and the mobility of the charge carriers. The conductivity due to charge carriers is small at low temperatures. Accordingly, the AC conductivity is expected to exhibit the observed frequency dependence (Fig. 5a), science it depends mainly on the polarization of immobile ions. The conductivity of the charge carriers is expected to increase with temperature [40]. At high temperature, the dominant factor in the conductivity will be the mobility of the charge carriers; while the polarization of the immobile ions will make a less significant contribution. Therefore, at high temperatures, the AC conductivity will have a lower dependence on frequency as shown in (Fig. 5b).

4 Conclusion

Copper containing nominal diopside ($Cu_{0.50}Ca_{0.75}Mg_{0.75}Si_2O_6$) glass, with or without Cr_2O_3 or TiO_2, was characterized by X-ray analysis and SEM. Since it was contains scattered clusters of nano-crystals of diopside, cuprite and tenorite.

The calculated activation energy measured at 100 kHz and 1 MHz in the region from 473 to 573 (K) of the glass samples lies in the range 0.55–0.98 (eV). The AC conductivity values of the studied glass samples indicated that the incorporation of Cr_2O_3 and TiO_2 results in higher conductivity values than those of the free glass sample. The magnitude of the σ_{ac} values

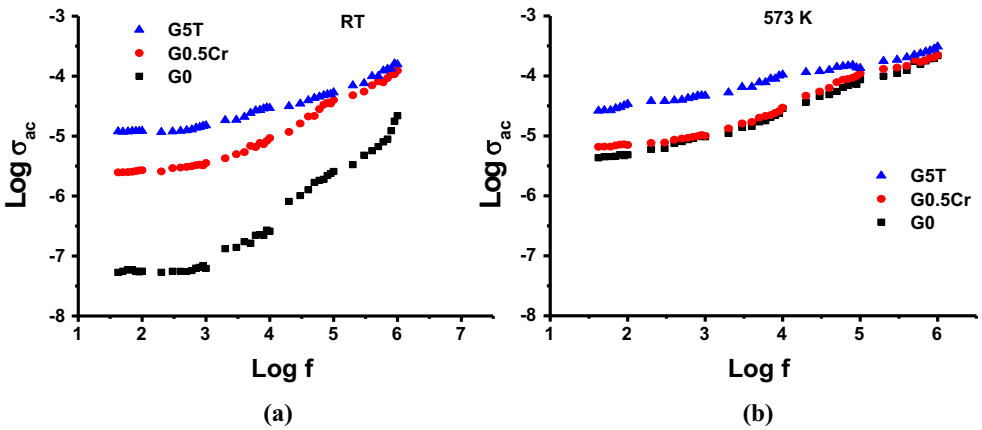

Fig. 5 Variation of AC conductivity (σ_{ac}) with frequency at: (a) room temperature and (b) 573 K

indicated that the electrical conductivity of such glasses lies in the range of semiconductors. The samples studied can be classified as one of the semiconductor categories that can be used at room temperature in electronic devices.

Acknowledgements The authors are grateful to the National Research Centre, the institution to which they belong, for providing the facilities that the current research required.

Code Availability Not applicable.

Authors' Contributions Reham M.M. Morsi, has carried out the AC conductivity measurements, their discussions and conclusions. Gehan T. El-Bassyouni and Esmat M. A. Hamzawy prepared the samples, their XRD, SEM and their discussions and conclusions. All the authors contributed in writing the original manuscript.

Data Availability Not applicable.

Declarations

Conflict of Interest The manuscript's authors declare that there are no conflicts of interest exist.

Ethics Approval Not applicable.

Consent to Participate Not applicable.

Consent for Publication Not applicable.

References

1. Nonami T, Tsutsumi S (1999) Study of diopside ceramics for biomaterials. J Mater Sci Mater Med 10:475–479
2. Si W, Li S (1676) Crystallization kinetics of diopside glass ceramics. J Phys Conf Ser 2020:012150
3. Myung WC, Soo HL, Ho SC, Jong ML (2009) Properties of glasses based on the CaO–MgO–SiO_2 system for low-temperature co-fired ceramic. Ceram Int 35:2513–2515
4. Abdel-Hameed SAM, El-kheshen AA (2003) Thermal and chemical properties of diopside-wollastonite glass-ceramics in the SiO_2–CaO–MgO system from raw materials. Ceramics International 29: 265–269
5. Alexander K, Lorenzo A, Ildiko M, Mario P (2004) Properties of sintered glass-ceramics in the diopside–albite system. Ceram Int 30: 2129–2135
6. Kleebusch E, Patzig C, Höche T, Rüssel C (2018) The evidence of phase separation droplets in the crystallization process of a Li_2O-Al_2O_3-SiO_2 glass with TiO_2 as nucleating agent – an X-ray diffraction and (S)TEM-study supported by EDX-analysis. Ceram Int 44: 2919–2926
7. Höche T (2011) $ZrTiO_4$ crystallisation in nanosized liquid- liquid phase-separation droplets in glass - a quantitative XANES studies. Cryst Eng Comm 13:2550–2556
8. Alharbi OA, Zaki DY, Hamzawy EMA (2012) Effect of TiO_2, LiF and Cr_2O_3 in the crystallization of cristobalite and tridymite in sintered glass-ceramics. Silicon 4(4):281–287
9. Gu SB, Mi JY, Woo GJ (2017) Effect of the Cr_2O_3 and TiO_2 as nucleating agents in SiO_2-Al_2O_3-CaO-MgO glass-ceramic system met. Mater Int 23:798–804
10. Li H, Liu S, Xu W, Zhang Y, Shi Y, Ma J, Ouyang S, Du Y (2021) The mechanism of the crystalline characteristics of spinel-induced epitaxial growth of diopside in CMAS glass-ceramics. J Eur Ceram Soc 41:1603–1612
11. Sycheva GA, Polyakova IG, Kostyreva TG (2016) Volumetric nucleation of crystals catalyzed by Cr_2O_3 in glass based on furnace slags. Glas Phys Chem 42:238–245
12. Reddy AA, Tulyaganov DU, Goel A, Pascual MJ, Kharton VV, Tsipis EV, Ferreira JMF (2012) Diopside - mg orthosilicate and diopside - Ba disilicate glass-ceramics for sealing applications in SOFC: sintering and chemical interactions studies. Int J Hydrogen Energy 37:12528–12539
13. Sabato AG, Rost A, Schilm J, Kusnezoff M, Salvo M, Chrysanthou A, Smeacetto F (2019) Effect of electric load and dual atmosphere on the properties of an alkali containing diopside-based glass sealant for solid oxide cells. J Power Sources 415:15–24
14. Liu W, Zhang H, Shi JA, Wang Z, Song C, Wang X, Lu S, Zhou X, Gu L, Louzguine-Luzgin DV, Chen M, Yao K, Chen N (2016) A room-temperature magnetic semiconductor from a ferromagnetic metallic glass. Nat Commun 7:13497
15. Han Y, Jia X, Liu F, Deng L, Zhang X (2019) Effect of Cr_2O_3 content on high-temperature dielectric properties and crystallisation of CMAS glass-ceramics. Mater Res Exp 6:075213
16. Jo HJ, Sun GN, Kim ES (2016) Enhanced crystallization behaviour and microwave dielectric properties of $0.9CaMgSi_2O_6$–$0.1MgSiO_3$ glass-ceramics doped with TiO_2. J Korean Ceram Soc 53(2):139–144
17. Li B, Wang S, Fang Y (2017) Effect of Cr_2O_3 addition on crystallization, microstructure and properties of Li_2O–Al_2O_3–SiO_2 glass-ceramics. J Alloys Compd 693:9–15
18. Kang B, Kang S (2020) Crystal growth behavior, nanometer microstructure, and mechanical properties of diopside-based glass-ceramics. J Nanosci Nanotechnol 20:183–189
19. Barbieri L, Leonelli C, Manfredini T, Pellacani GC, Siligardi C, Tondello E, Bertoncello R (1994) Solubility, reactivity and nucleation effect of Cr_2O_3 in the CaO-MgO-AI_2O_3-SiO_2 glassy system. J Mater Sci 29:6273–6280
20. Hamed G, Rahmatollah E, Shaghayegh HJ (2015) Preparation of nanostructure bioactive diopside scaffolds for bone tissue engineering by two near net shape manufacturing techniques, December 2015. Mater Lett 167:157–160
21. Alekseev YI, Galanov YI (1990) Electrical conductivity of diopside ceramics. Glas Ceram 47:24–26
22. Morsi MM, Margha FH, Morsi RMM (2018) Effect of sintering temperature on the developed crystalline phases, optical and electrical properties of $5ZnO$-$2TiO_2$- $3P_2O_5$ glass. J Alloys Compd 769: 758–765
23. EL-Desoky MM, Hassaan MY, El-Kottamy MH (1998) WO_3 concentration and frequency dependence of conductivity and dielectric constant of sodium borate tungstate glasses. J Mater Sci Mater Electron 9:447–451
24. Ekarat M (2010) Redox behavior of glasses doped with copper and arsenic, antimony or tin, Ph.D Thesis, der Chemisch-Geowissenschaftlichen Fakultät der Friedrich-Schiller-Universität Jena, Germany
25. Prabu RD, Valanarasu S, Ganesh V, Shkir M, AlFaify S, Kathalingam A, Srikumar SR, Chandramohan R (2018) An effect of temperature on structural, optical, photoluminescence and electrical properties of copper oxide thin films deposited by nebulizer spray pyrolysis technique. Mater Sci Semicond Process 74:129–135

26. Basha MAF, Morsi RMM, Morsi MM, Basha AF (2019) The magnetic, electrical and optical properties of rare earth Er^{3+} doped Lead borate glass. J Electron Mater 48(10):6686–6693
27. Ladhar A, Arous M, Kaddami H, Raihane M, Kallel A, Graça MPF, Costa LC (2015) AC and DC electrical conductivity in natural rubber/nanofibrillated cellulose nanocomposites. J Mol Liq 209: 272–279
28. Langar A, Sdiri N, Elhouichet H, Ferid M (2017) Structure and electrical characterization of ZnO-Ag phosphate glasses. Results Phys 7:1022–1029
29. Zeyada HM, Youssif MI, El-Ghamaz NA, Aburoj MS (2015) Electrical conduction mechanisms and dielectric constants of nanostructure zinc indium selenide thin films. Scientific Journal for Damietta Faculty of Science 4(2):79–89
30. Qiang Z, Guorong C, Guoping D, Danping C (2009) The reduction of Cu^{2+} to Cu^{+} and optical properties of Cu^{+} Ions in Cu-doped and Cu/Al-Codoped high silica glasses sintered in an air atmosphere. Chem Phys Lett 482(s 4–6):228–233
31. Li JW, Ji PY, Kuo CC, Seshadri ST (2015) Effects of MgO and Al_2O_3 addition on redox state of chromium in CaO-SiO_2-CrO_x slag system by XPS method. J Am Ceram Soc 91(11):3571–3579
32. Hichem K, Renaud P, Christophe R, Michel V (2008) Redox-control solubility of chromium oxide in soda-silicate melts. J Am Ceram Soc 91(11):3571–3579
33. Sanjay NK, Agarwal AA (2010) Study of structural, optical and transport properties of semiconducting Fe_2O_3-PbO-B_2O_3. Indian J Pure Appl Phys 48:205–211
34. Doweidar H, El-Damrawi G, Abdelghany M (2012) Structure and properties of CaF_2–B_2O_3 glasses. J Mater Sci 47:4028–4035
35. Nobuhito I, Yusuke OI, Gin-ya A (2000) Divalent magnesium ion conducting characteristics in phosphate based solid electrolyte composites. J Mater Chem 10:1431–1435
36. Michael S, Mackenzie JD (1996) Ionic conductivity in calcium silicate glasses. J American Ceramic Soc 49:582–585
37. Khater GA, Nabawy BS, Kang J, Mahmoud MA (2019) Dielectric properties of basaltic glass and glass-ceramics: modeling and applications as insulators and semiconductors. Silicon 11:579–592
38. Morsi RMM, Basha MAF, Morsi MM (2016) Synthesis and physical characterization of amorphous silicates in the system SiO_2-Na_2O– RO (R = Zn, Pb or Cd). J Non-Cryst Solids 439:57–66
39. Shaaban MH (1998) The ac conductivity of CuO-containing lead silicate glasses. J Mater Sci Mater Electron 9:55–60
40. Margha FH, El-Bassyouni GT, Turky GM (2019) Enhancing the electrical conductivity of vanadate glass system (Fe_2O_3, B_2O_3, V_2O_5) via doping with sodium or strontium cations. Ceram Int 45:11838–11843